

GIS-based rockfall susceptibility zoning in Greece

Charalampos Saroglou

Department of Geotechnical Engineering, School of Civil Engineering, National Technical
University of Athens, e-mail: saroglou@central.ntua.gr

Abstract

The assessment of rockfall risks on human activities and infrastructure is of great importance. Rock falls pose a significant risk to a) transportation infrastructure b) inhabited areas and c) Cultural Heritage sites. The paper presents a method to assess rockfall susceptibility at national scale in Greece, using a simple rating approach and GIS techniques. An extensive inventory of rockfalls for the entire country was compiled for the period between 1935 and 2019. The rockfall events that were recorded are those, which have mainly occurred as distinct rockfall episodes in natural slopes and have impacted human activities, such as roads, inhabited areas and archaeological sites. Through a detailed analysis of the recorded data, it was possible to define the factors which determine the occurrence of rockfalls. Based on this analysis, the susceptibility zoning against rockfalls at national scale was prepared, using a simple rating approach and GIS techniques.

The rockfall susceptibility zoning takes into account the following parameters: a) the slope gradient, b) the lithology, c) the annual rainfall intensity, d) the earthquake intensity and e) the active fault presence.

Emphasis was given on the study of the earthquake effect as a triggering mechanism of rockfalls. Finally, the temporal and spatial frequency of the recorded events and the impact of rockfalls on infrastructure assets and human activities in Greece were evaluated.

29 **Keywords**

30 Rockfall, susceptibility, GIS, rainfall, earthquake, fault, inventory.

31 **1. INTRODUCTION**

32 The assessment of rockfall risks on human activities and infrastructure is of great
33 importance. Rock falls pose a significant risk to a) transportation infrastructure b)
34 inhabited areas and c) Cultural Heritage sites. The main triggering factors are rainfall,
35 earthquakes and thermal expansion – contraction. Geological assessment leads to
36 accurate prediction of the outbreak of such events, explains its mechanism of
37 occurrence and assists in the effective design of protection measures.

38 In the last decade, Geographic Information Systems (GIS) were used for creating
39 spatial models of potential hazard zonation maps for civil engineering and protection
40 purposes by Mason and Rosenbaum (2002), Mancini et al. (2010) and Calvello et al.
41 (2013). Several authors have presented the important role of GIS in hazard
42 assessment and mitigation; these include Carrara et al. (1991), Barredo et al. (2000),
43 Fernandez et al. (2003), Kolat et al. (2006), Yilmaz and Yildirim (2006), Nandi and
44 Shakoor (2009), Paulin et al. (2014) and others.

45 Susceptibility is the likelihood that an event will occur in a specific area based on the
46 local terrain conditions (Brabb, 1984). The susceptibility describes the predisposition
47 of an area to be affected by a given future event and results in an estimate of where
48 rockfalls are likely to occur (Guzzetti 2006). According to Ferrari et al. (2016),
49 susceptibility can be assessed by: a) Geomorphological mapping, b) Empirical and
50 semi-empirical rating systems, c) Statistical analyses and d) Deterministic methods.

51 The resulting susceptibility maps illustrate the predisposition towards instability of a
52 slope or area. According to Fell et al. (2008), rockfall susceptibility may be assessed
53 based on either qualitative or quantitative approach. The qualitative approach is
54 based on either field geomorphologic analysis or the combination/ overlying of index

55 maps with or without weighting. In the present study, a semi-empirical rating was
56 used using overlying of index maps without weighting.

57 Chau et. al. (2003) and Chau et. al. (2004) presented a rockfall susceptibility map
58 based on a rockfall inventory for Hong Kong using GIS-based techniques at national
59 level. Carman et al. (2011) prepared a similar map for Slovenia. Trigila et al. (2013)
60 have presented a landslide susceptibility mapping at national scale in Italy using the
61 Italian landslide inventory. Günther et al. (2013) have presented landslide
62 susceptibility assessment for Europe. In Greece, Koukis et al. (2005) and
63 Sabatakakis et al. (2013) proposed a landslide hazard zonation and a landslide
64 susceptibility zonation using a landslide inventory derived from historical archives.
65 Antoniou & Lekkas (2010) prepared a rockfall susceptibility map for Santorini Island
66 in Greece using GIS methods. From the pertinent literature review, it is evident that
67 there is no rockfall susceptibility zonation available in Greece.

68 The geological structure of Greece (frequent occurrence of rock formations,
69 existence of faults and intense fracturing of rockmasses), the steep topography as
70 well as its high seismicity, contribute to the outbreak of rockfalls. During the last
71 decades, rockfalls in Greece are becoming a frequent phenomenon due to intense
72 rainfall events, earthquakes but also due to the extension of human activities in
73 mountainous areas. Earthquake-triggered rockfalls were specifically investigated in
74 the present study since historical and recent earthquakes in Greece have triggered a
75 significant number of rockfalls, as reported by Papazachos & Papazachou (1997),
76 Pavlides & Caputo (2004), Ambraseys & Jackson (1990) and Saroglou (2013). More
77 recently, Papathanassiou et al. (2013) investigated the earthquake induced
78 instabilities in Lefkada Island and Zygouri & Koukouvelas (2015) have studied the
79 evolution of rockfalls triggered by earthquakes in northern Peloponnese. Saroglou et
80 al. (2017) studied the co-seismic rockfalls during Lefkada (2015) and Cephallonia

(2014) earthquakes and Saroglou et al. (2018) back-analysed a coseismic rockfall trajectory of the Lefkada 2015 earthquake using UAV-based mapping.

The paper presents an extensive inventory of rockfalls for the period between 1935 and 2019 with events, which have mainly occurred in natural slopes and have impacted human activities, such as roads, inhabited areas and archaeological sites. Rockfalls that have occurred in man-made slopes were not taken into account in the present inventory. The paper also presents a method to assess rockfall susceptibility of natural slopes at national scale in Greece, using a simple rating approach and GIS techniques. The susceptibility map was based on simple rating of specific factors: a) slope gradient, b) lithology, c) rainfall intensity, d) earthquake intensity and e) active fault presence. These factors were selected based on the analysis and evaluation of the rockfall data recorded in the inventory of main rockfall events in Greece between 1935 and 2019. The importance of each factor in relation to the occurrence of rockfalls was investigated.

In the next sections, the rockfall inventory is first presented followed by the susceptibility assessment using GIS. The spatial distribution of rockfall events is evaluated in comparison to the susceptibility map.

2. ROCKFALL INVENTORY

A rockfall inventory was created for Greece for the period between 1935 and 2019. Sixty (60) rockfalls events were recorded in forty three (43) sites, as presented in the national map of Greece shown in Figure 1.

The rockfall events that were recorded are those, which have mainly occurred as distinct rockfall episodes in natural slopes and have impacted human activities, such as roads, inhabited areas and archaeological sites. Rockfalls, which have occurred in man-made slopes (mainly along highways), were not taken into account in the present inventory.

The following data were recorded for each rockfall episode: a) Location, b) Coordinates, altitude, c) Type of site (roadway, inhabited area, archaeological site), d) Date (s) of rockfall event(s), d) Triggering mechanism (rainfall, earthquake, other), e) Fault presence (slope scarp), f) Geological formation, g) Rock mass type, degree of fracturing, h) Slope height, i) Slope angle, j) Block size of fallen blocks, k) Impact (type of affected site), l) Presence of vegetation (forest etc.), m) Energy level.

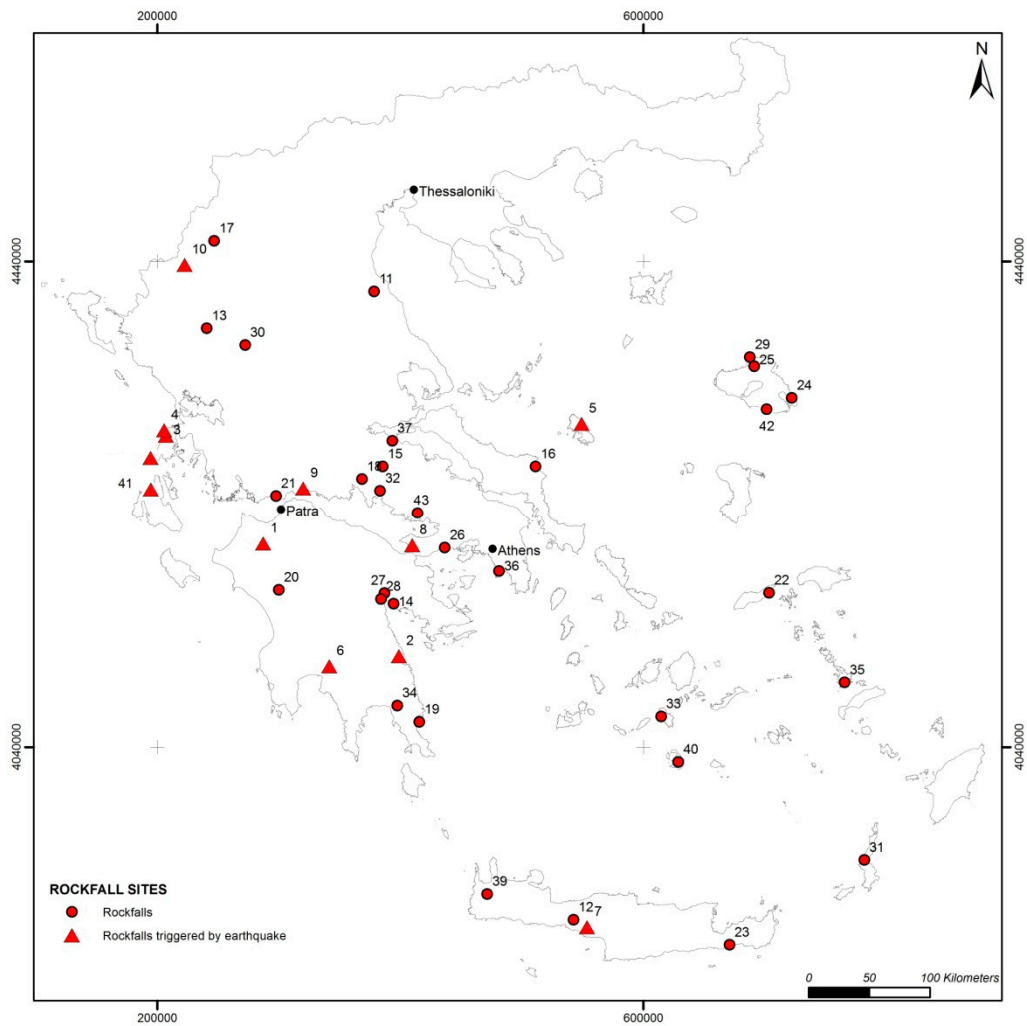


Figure 1. Inventory of recorded rockfall events in Greece

The main recorded parameters of these events are given in Table 1. More details for this rockfall inventory and sources of records were reported in Saroglou (2013).

In some sites, more than one event has occurred and thus it is possible to predict the return period of rockfalls in these cases.

Koukis & Ziourkas (1991) and Koukis et al. (2005) presented a landside frequency zonation map for Greece. The relative frequency of rockfalls, expressed in cases per surface area, in these maps was 11 %. The maximum frequency of landslides is along the Pindos geotectonic zone, where a large number of slope instabilities occur in the flysch formation in the form of soil type or composite failures (rotational, translational etc.). Based on the present study, the maximum frequency of rockfalls is encountered in western and central Greece.

Rockfalls are generally more frequent in mountainous areas in Greece, where the slope angle is greater than 50 degrees. This is evidenced by the higher occurrence of events in mountainous areas of Greece, such as Pindos and Parnassos Mountain (Figure 1). Rockfalls also occur in low to medium altitude areas where slopes with steep morphology exist, usually related to fault scarps, such as the case of Kakia Scala (Table 1, site26), Klokova (site 21) and Monemvasia promontory (site 19).

Table 1 – Main data of recorded rockfalls in Greece

Id	Location	Type	Date	Trigger	Rock type	Fault scarp	Block (m³)	Impact
1	Santomeri, Achaia	D	8/6/2008	E (6.5)	L	Y	4	DH
2	Leonidio, Tiros	R	6/1/2008	E	L	Y	<1	RC
3	Drimonas, Lefkada	D/R	14/8/2003	E (6.4)	L	Y	< 1	DR
4	Lefkada, Ag.Nikitas	D/R	14/8/2003 19/11/2015	E (6.4) E (6.5)	L	Y	13.7 2	PDR HLL
5	Skyros Island	A	26/7/2001	E (5.8)	L	Y	1-2	DC
6	Ladas, Eleochoi, Poliani, Kalamata	D	13/9/1986	E (6.2)	L		<1	PDH
7	Heraklion (Pitsidia, Akoumia)	D	14/5/1959	E (6.3)	L	Y	<1	DH
8	Geraneia Mt.		24/2/1981	E (6.3)	L	Y		
9	Itea, Monastiraki	R	18/1/2010	E (5.1)	L	Y	<1	DR
10	Konitsa, Ioannina	D/A	8/1998	E	LA		2	DH
11	Tempi Valley	R	17/12/2009 2004, 1977 ¹	ND	M		0.5 – 5, 50	HLL, RC
12	Kourtaliotis gorge	R	4/3/2012	R	L	Y	1	DR
13	Pramanta -	R	9/3/2004	ND	L	Y	< 1	DR

Id	Location	Type	Date	Trigger	Rock type	Fault scarp	Block (m³)	Impact
	Ioannina							
14	Acronafplia	A	1/2010	ND	L		0.5	V
15	Tithorea, Parnassos	D	19/12/2010 1999, 1957	ND	L		10	DH
16	Oksilithos, Kymi	R	13/8/2008	ND	MS		1.5	HI
17	Eptachori, Kastoria	D	1935, 51, 68, 70, 87, 93, 94	R	M	Y	336 ²	DH
18	Delfi ancient site	A	2003, 09 ¹	R	L		8	V
19	Monemvasia	A	2003, 2010 ¹	R	L	Y	2	DH, V
20	Anc. Olympia	R	22/1/2013	R	L		0.5	DR
21	Klokova Mt.	R	16/11/2012	ND	L		1-2	DR
22	Therma Ikaria	D	10/1978	ND	M	Y	1	PDH
23	Ag. Fotia, Crete	R	-	ND	S		<1	DR
24	Taxiarches, Lesvos	D	1963, 3/11/09	ND	M	Y	1	DH
25	Mythimna, Lesvos	A	2001	R	A		0.3	ND
26	Kakia Scala	R	20/11/2000	R	L	Y	0.5	HLL
27	Argos Castle	A	1987	ND	L			D
28	Kefalari, Argos	D	20/4/2012	ND	L	Y	0.1	HLL
29	Stypsi, Lesvos	D	1963, 1977	R	A		0.5- 3.0	DH
30	Orliagas, Ziakas	D/R		ND	L	Y	1	ND
31	Carpathos, Akropoli	D	-	ND	L			-
32	Vageni Distomo	D/R		ND	C	Y	40	PDR
33	Kalymnos	D	12/2002	R	L		4	PDH
34	Molaoi, Lakonia	D	2/2003	R	CA		1-2	PDH
35	Chora, Ios	D	-	ND	S		1	PDH
36	Vouliagmeni, Attica	D	1/1982	ND	L	Y	1-2	
37	Kamena Vourla	D	27/8/2012	ND	L		1	DH
38	Nea Pefki, Trikala	R	20/10/2010	R	S		< 1	DR
39	Topolia, Chania	R	23/2/2012	R	L	Y	0.5	FB
40	Santorini	D	2011	R	P		0.5	HLL
41	Myrtos, Cephallonia Island	O	17/1/2014	E (6.1)	L	Y	50	DR
42	Lesvos, Plomari	D	24/11/2018	R	SG		10	DH
43	Alyki, Voiotia	D	27/1/2019	R	L		70	DH

¹ More rockfall events exist, which are not presented here, ²the largest rock block, 15 smaller rocks have fallen in this site, Type: R=Roadway, D=Domestic, A: Archeological, O=other (touristic area, coast), Trigger: R=rainfall, E=Earthquake, ND=Not defined, Rock type: L= limestone, M=marble, CA= Calcitic agglomerate, LA=Limestone agglomerate, C= conglomerates, S=sandstone, M=marls, MS= marls/ sandstones, SG=Schist/gneiss, A= Andesite, P= Pyroclastics, Fault Scarp: Y=yes, Impact: HLL= Human loss, HI=Human injury, V=Potential impact on visitors, damage to archaeological site, DH=Damage to houses, PDH=Potential house damage, RC=Roadway closure, DR=Damage on roadway, PDR=Potential roadway damage, FB=fall on moving bus, DC=Damage on cars, ND= No damage.

3. EVALUATION OF THE ROCKFALL INVENTORY

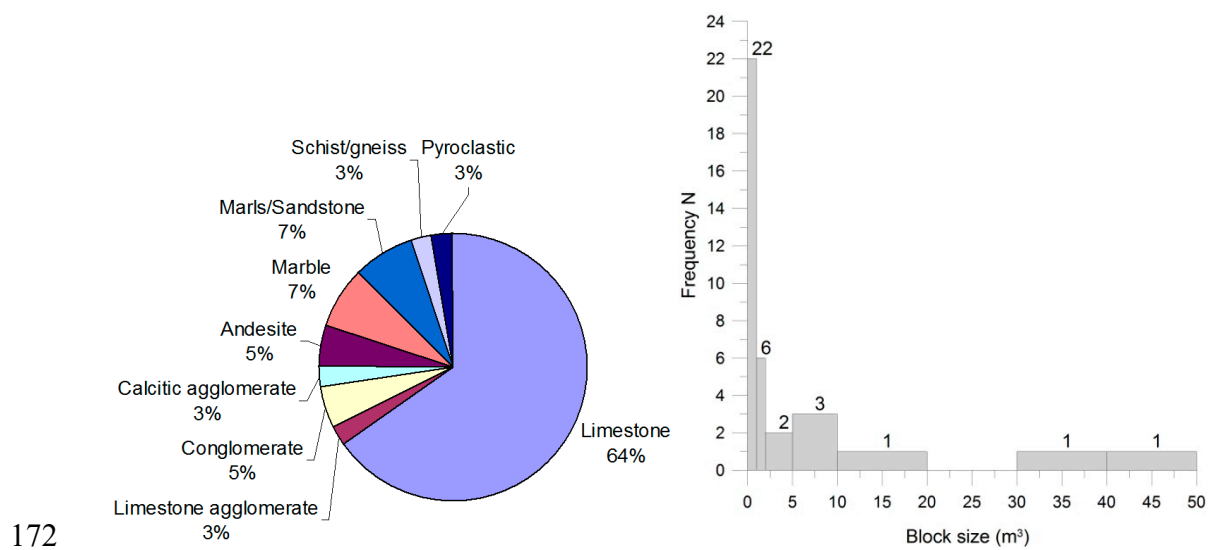
3.1. Geological framework and rockfalls in Greece

The most frequent geological formation encountered in the study areas, is limestone (frequency of occurrence equal to 64%). The occurrence of the rocks forming the slopes, recorded in the database, is presented in Figure 2a. The most frequent geological formation encountered in the rockfall study areas, is limestone (with a frequency equal to 64%), while in fewer sites marble (7%), marls/sandstones (7%), schists/gneisses (3%) and igneous rocks (8 %) is encountered.

Generally, limestones are found broken to heavily broken, especially when in the vicinity of faults, resulting in blocky rock masses. Rockfalls are favoured in blocky or very blocky rock masses, since medium to large rock blocks are formed by intersecting discontinuities and can be relatively easily detached by the action of water or seismic loading.

In a large number of sites, scree is present at the foot of the slopes. The presence of a scree slope at the base of the rock cliff suggests slope ravelling activity. According to Sartori et al. (2003), this activity can be linked to the progressive failure of the rock cliff, but can also be a precursory event of larger rockfalls. Marquinez et al. (2003) presented a rockfall activity index defined as the ratio A_t / A_r , which correlates with the ability of a certain lithology to produce rockfalls. The index is the ratio of the cartographic surface of the recent talus scree (A_t) to that of the rocky slope acting as source area (A_r). Dorren & Seijmonsbergen (2003) assigned rockfall susceptibility categories to geological formations according to their nature and ability to produce rocks blocks. They considered limestone to have high susceptibility, while schists, slates, marls and sandstones low to medium. The block size of the fallen blocks ranges between 0.5 m³ and 50 m³ with an exception of Eptachori rockslide. The

170 blocks size is less than 1 m^3 in 22 sites and between 1 and 5 m^3 in 8 sites, as
 171 presented in Figure 2b.



173 Figure 2. a) Lithology in areas of rockfall events, b) Frequency of block size of fallen
 174 rocks

175 3.2. Temporal – spatial frequency of rockfalls

176 Based on the recorded data, it was possible to define the frequency of rockfalls for
 177 the considered time period. The average frequency is one event every 1.3 years,
 178 considering the total number of events, irrespective of the rockfall magnitude. For
 179 rockfalls with volume of blocks less than 2.5 m^3 the return period is 2.8 years, while
 180 for events with volume greater than 10 m^3 the return period is 16 years. The
 181 frequency of rockfalls is shown in Figure 3. It is noted that the number of rockfalls has
 182 increased in the 2000- 2010 and 2010- 2020 decades, which may be attributed to
 183 reasons related with climate change (more extreme weather events) or increase of
 184 knowledge of rockfall outbreaks through improvement of communication systems.

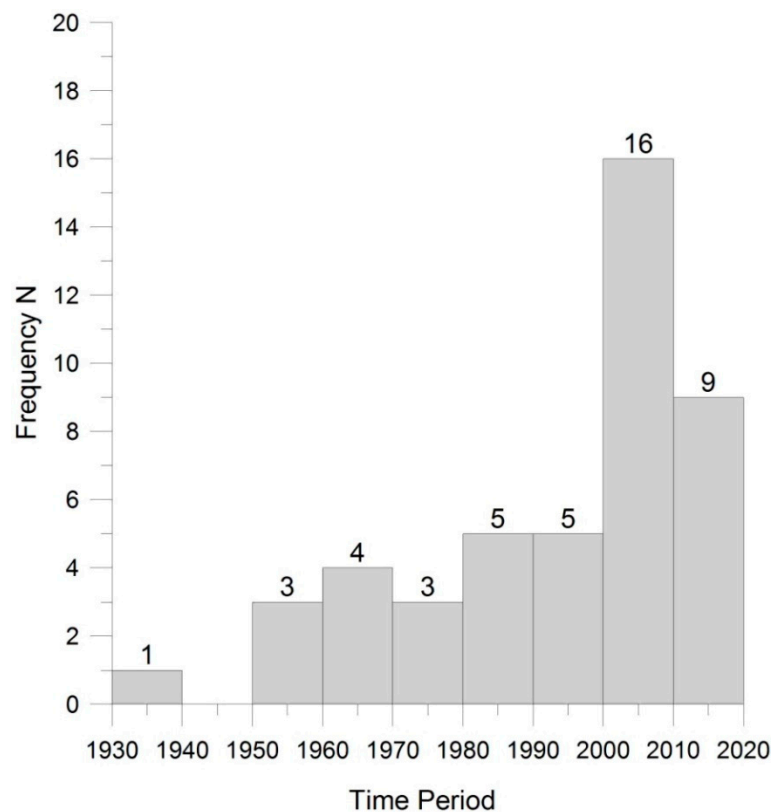


Figure 3. Frequency of rockfalls for the period between 1935 and 2019.

3.3. Triggering mechanisms

According to the evaluation of the recorded data, the main triggering mechanism of rockfalls is rainfall. Thirteen (13) rockfall events were triggered by rainfall (frequency equal to 33%) and one (1) event by a snowfall. An increase in the number of rockfalls, triggered due to rainfall, has occurred during the last decade mainly due to the occurrence of extreme weather events during the winter periods. This is evidenced, by the occurrence of eighty six (86) instability phenomena (5% of these were rockfalls) in 2010 (Nikolaou et. al., 2011), 95 % of which were triggered by intense rainfall during February and November-December period.

The second most important triggering mechanism was seismic loading as twelve (12) rockfall events were triggered during earthquakes (frequency equal to 25%).

3.4. Coseismic rockfalls in Greece

Earthquakes, which triggered large rockfall events, are those during Alkyonides (1981) and Kalamata (1986) earthquakes, in Skyros Island (2001), in Achaia (2008), in Cephallonia Island (2014) and in Lefkada Island (2003 and 2015). During some of these earthquakes, such as the ones in Kalamata and Achaia, rockfalls occurred along reactivated fault scarps.

The most significant coseismic rockfalls in Greece, since 1980, are presented in Table 2, where the location, the date, the magnitude (M_w) of the earthquake and the distance of the rockfall site from the earthquake epicenter are reported.

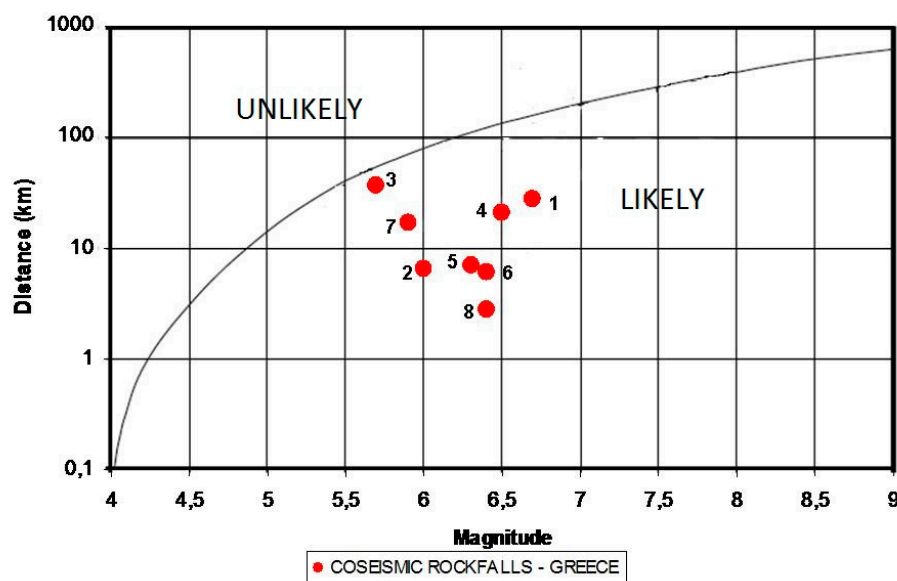
Table 2. Main coseismic rockfalls in Greece

No.	Location	Date	Magnitude (M_w)	Rockfall site	Distance (km)
1	Gerania, Korinthos	13/9/1986	6.7	Alkyonides	27
2	Kalamata	8/1998	6	Kalamata-Sparti road	6.5
3	Konitsa	14/8/2003	5.7	Eptachori	36.8
4	Skyros	24/2/1981	6.5	Skyros castle	20.5
5	Lefkada	26/7/2001	6.3	Ag. Nikitas	7
6	Achaia	8/6/2008	6.4	Santomeri	5.9
7	Cephallonia	26/01/2014	5.9	Myrtos	16.4
8	Lefkada	11/2015	6.4	Ag. Petros	2.8

The effect of earthquakes on the occurrence of rockfalls is twofold: a) the magnitude and epicenter distance of an earthquake define whether an unstable block will be detached from a rock slope and b) the peak ground velocity exerted by an earthquake determines the displacement magnitude of a rock block. Hazard assessment methodologies against earthquake-triggered rockfalls have been applied by Gorum et al. (2011) for the Wenchuan earthquake-induced landslides, by Wasowski & Del Gaudio (2000) in Italy, by Rodriguez-Peces et al. (2011) in Spain and Marzorati et al. (2002), who produced a rockfall susceptibility map triggered by earthquakes in the Umbria and Marche region in Italy.

217 Keefer (1984) and Rodriguez et al. (1999) developed a magnitude – source distance
 218 diagram for landslides, which can also be applied to rockfalls. This diagram (Keefer,
 219 1984) is presented in Figure 4, in which the main coseismic rockfalls from Greece are
 220 plotted. The dashed curve presents the maximum distances from fault rupture zones
 221 at which disrupted slides and falls have been observed worldwide. Magnitude–
 222 distance relations for earthquake-induced landslides in Greece have been proposed
 223 by Papadopoulos & Plessa (2000). More recently, Chousianitis et al. (2016)
 224 performed an assessment of the earthquake-induced landslide hazard in Greece,
 225 investigating the arial intensity and spatial distribution of slope resistance demand.

226 The triggering of rockfalls for the events whose epicentral distances plot above the
 227 threshold curve is unlikely.



228

229 **Figure 4.** Magnitude – source distance diagram of coseismic rockfalls in Greece

230 It is obvious, that all the coseismic rockfall events in Greece plot well below the curve
 231 suggested by Keefer (1984). The magnitude of earthquakes that triggered rockfalls is
 232 between $M_w = 5.7$ and 6.7 , while the maximum distance from the epicenter to a
 233 reported rockfall was 36.8 km.

234 3.5. Impact of rockfalls in Greece

Based on the analysis of the data, the main impact of rockfalls is damage and temporary closure of roadways (frequency equal to 32%) and secondly damage to houses (frequency equal to 20%). The percentage of potential damage to roadways and houses is 5% and 13% respectively. The potential damage is defined when a rockfall event poses a direct impact to houses or roadways, but has not impacted them already. Additionally, the percentage of loss of human life is 11%, which is considered exceptionally high. Furthermore, the frequency of potential impact on visitors and damage to archaeological sites is equal to 11%.

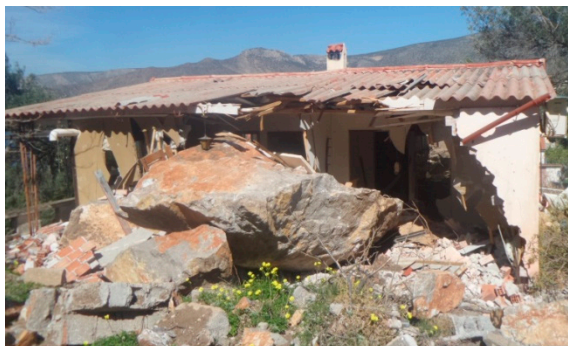
The most known and studied events, which have occurred along highways and other roads, are those of Tempi highway (shown in Figure 5b), Kakia Skala (site 26) and Klokova area (site 21). Significant rockfall events impacting roads have taken place in Ag. Nikitas in Lefkada island during the earthquakes in 2003 and 2015 (Figure 5b).



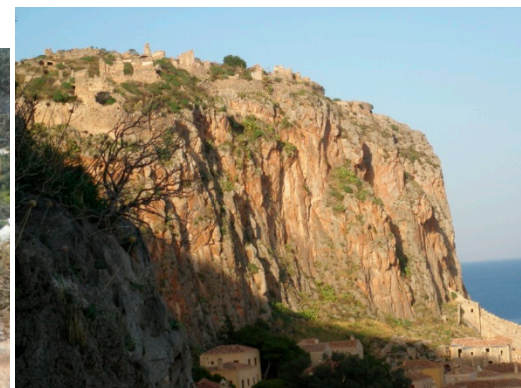
a)



b)



c)



d)

Figure 5. Impact of main rockfall events: a) on local road network in Lefkada during 2003 earthquake (site 3) b) on National Highway in Tempy valley in 2009 (site 11), c) in Alyki village in 2019 (site 43), d) in Monemvasia archaeological site (site 19).

Recent events that affected inhabited areas, are those in Eptachori in 1994 (site 17), in Skyros in 2001 (Marinos & Tsiambaos, 2002), Santomeri in 2008 (Koukouvelas et al., 2015) and Tithorea in 2010 (Saroglou et. al., 2015), Plomari in 2018 and Alyki village in 2019.. Finally, a house was impacted by a rockfall during a M_w 6.4 earthquake in Lefkada in 2015, resulting in one casualty (Saroglou et. al., 2018).

Sites of high risk in inhabited areas need to be identified in order to minimize rockfall risk. Additionally, there are a large number of rockfall incidents, which have occurred in archaeological sites. These pose a significant danger to tourists and visitors and affect the integrity of the monuments. Such an example is the archaeological site of Delphi (Christaras & Vouvalidis, 2010) where part of the archeological site was closed in 2009. Other affected cultural heritage sites are Mythimna castle (Marinos et. al., 2002) and Monemvasia castle (Saroglou et al., 2012), as indicated in Figure 5d.

4. ROCKFALL SUSCEPTIBILITY

4.1. INTRODUCTION

In order to develop the rockfall susceptibility map, GIS techniques in combination with a simple rating approach were used. The main assessment factors were selected based on the evaluation of the recorded data presented earlier. These factors are the following: (1) slope gradient (2) lithology, (3) annual rainfall intensity, (4) earthquake intensity and (5) active fault presence.

The proximity of a fault has been taken into account only as a qualitative parameter, since it relates to the formation of steep rock cliffs and increased degree of fracturing of rockmass, thus it can be connected to the susceptibility of a rock slope to rockfalls.

Based on these factors, thematic maps for each factor were generated. The rating approach for each factor is described in the following paragraphs.

4.2. SUSCEPTIBILITY FACTORS

4.2.1. Slope gradient

Rock slope instabilities occur in steep slopes. The adopted cut off value for slope gradient, above which rock slope instability may occur, is 45° , by analogy with other approaches that give higher values to steeper slopes (Gupta et al., 1999; Meisina et al., 2001).

Based on the inventory, the slope angle in the areas with rockfall events, ranged between 45 and 90 degrees while the average slope angle was 70 degrees.

In the present study, a value of 27° was selected. If a value of 45° were to be chosen, the potential rockfall prone areas would be very limited due to the small scale of the map used (1:500.000). The DEM was provided by the Hellenic Military Geographical Service (HMGS) in form of 25 m density grid of elevation points. A Digital Elevation Model (DEM) with a spatial resolution of 25 m was created in ARCGIS. The standard ArcView processing was used (Ballifard et al., 2003), which is considered as more appropriate for rough surfaces. The rating for slope gradient is 1 for slopes with angle greater than 27° and 0 for slope angle less than 27° . The slope map is presented in Figure 6.

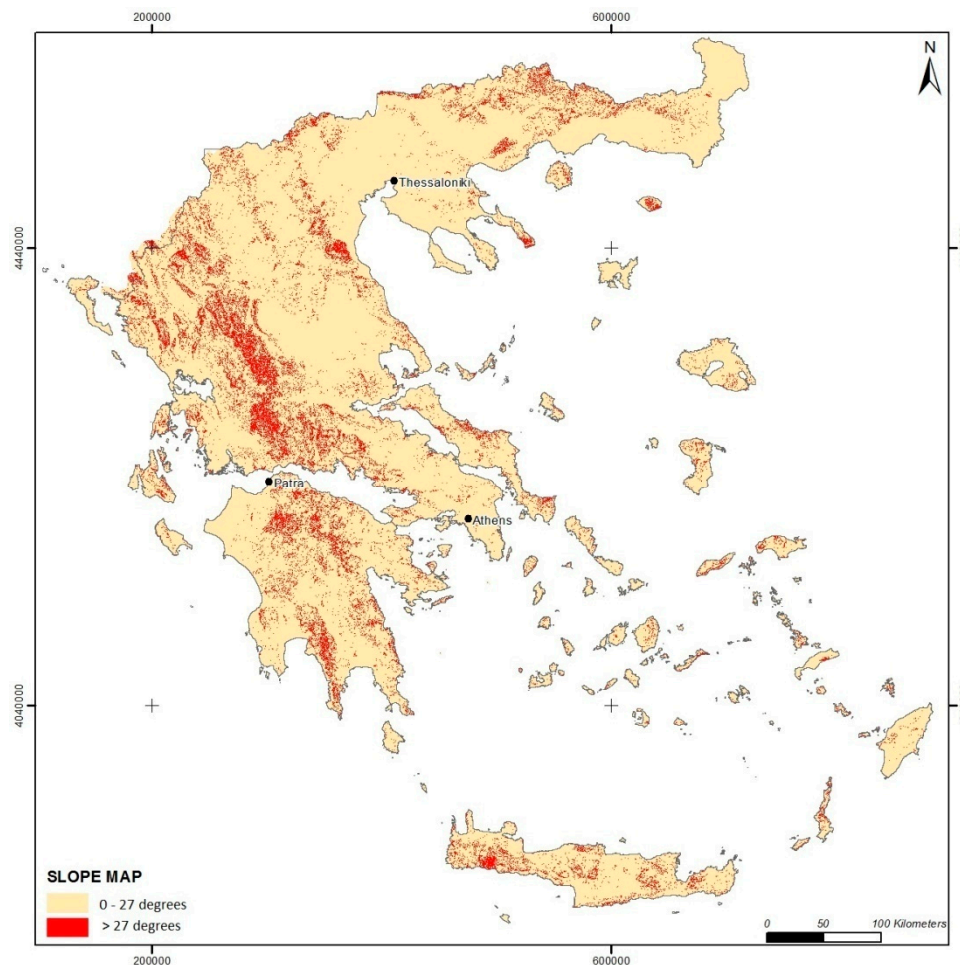


Figure 6. Slope map of Greece

4.2.2. Lithology

Lithology is a significant factor of the occurrence of rockfalls, since it controls the overall behaviour of the geological formation, the degree of fracturing; the permeability of the rockmass and in some occasions the steepness and height of the slope. Rockfalls are favoured in blocky or very blocky rock masses, since medium to large rock blocks are formed by intersecting discontinuities and can be relatively easily detached by the action of water or seismic loading.

Dorren & Seijmonsbergen (2003) proposed a rockfall susceptibility of geological formations and assigned rockfall susceptibility categories to them according to their nature and ability to produce rocks blocks. They considered that limestone has high susceptibility to generating rockfalls, while schists, slates, marls and sandstones low

309 to medium. Coe & Harp (2007) presented the influence of tectonic folding on rockfall
310 susceptibility suggesting that the presence of folds in limestone rocks increases the
311 number of rockfall events. Fityus et al. (2013) performed a detailed study on the
312 significance geological environment (mainly lithology and tectonic setting) on the
313 morphology and size of potentially unstable blocks.

314 In the present study, the basic data used to generate the original geological map in
315 vector format were obtained: from the existing geological map of Greece published
316 by the Institute of Geology and Mineral Exploration (scale 1:500.000). The main
317 geological formations were grouped into eleven (11) categories based on their
318 lithology, origin and engineering geological behavior (Figure 7). These were rated
319 with reference to their rockfall susceptibility, thus their ability to produce abundance
320 of rock blocks based on the usual rockmass structure conditions and behaviour
321 encountered in these categories. The rating was also based on the evaluation of the
322 rockfall inventory, presented earlier. The susceptibility rating of lithology is presented
323 in Table 3.

324 The lithology classification map is presented in Figure 8.

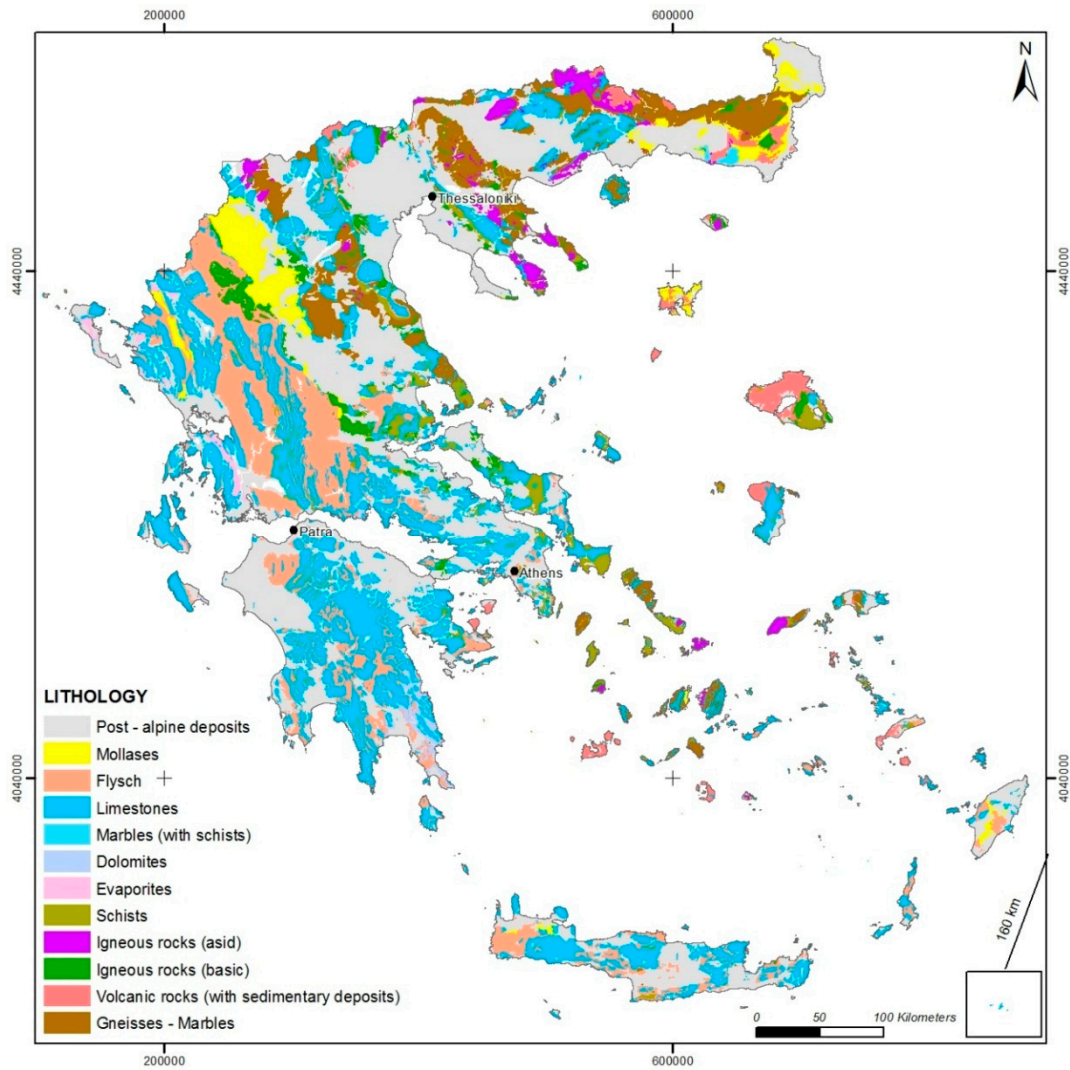


Figure 7. Main geological units encountered in Greece.

Table 3. Rating of lithology

Geological formation	Rockfall susceptibility	Class
Postalpine (Marls, claystones, etc.)	Low	3
Gypsum	Low	3
Schists	Low	3
Molasse deposits	Moderate	2
Flysch	Moderate	2
Igneous rocks (granites etc.)	Moderate	2
Marble – Schist (alternations)	Moderate	2
Dolomites	High	1
Limestone	High	1
Volcanic sedimentary rocks	High	1
Gneiss -Marbles	High	1

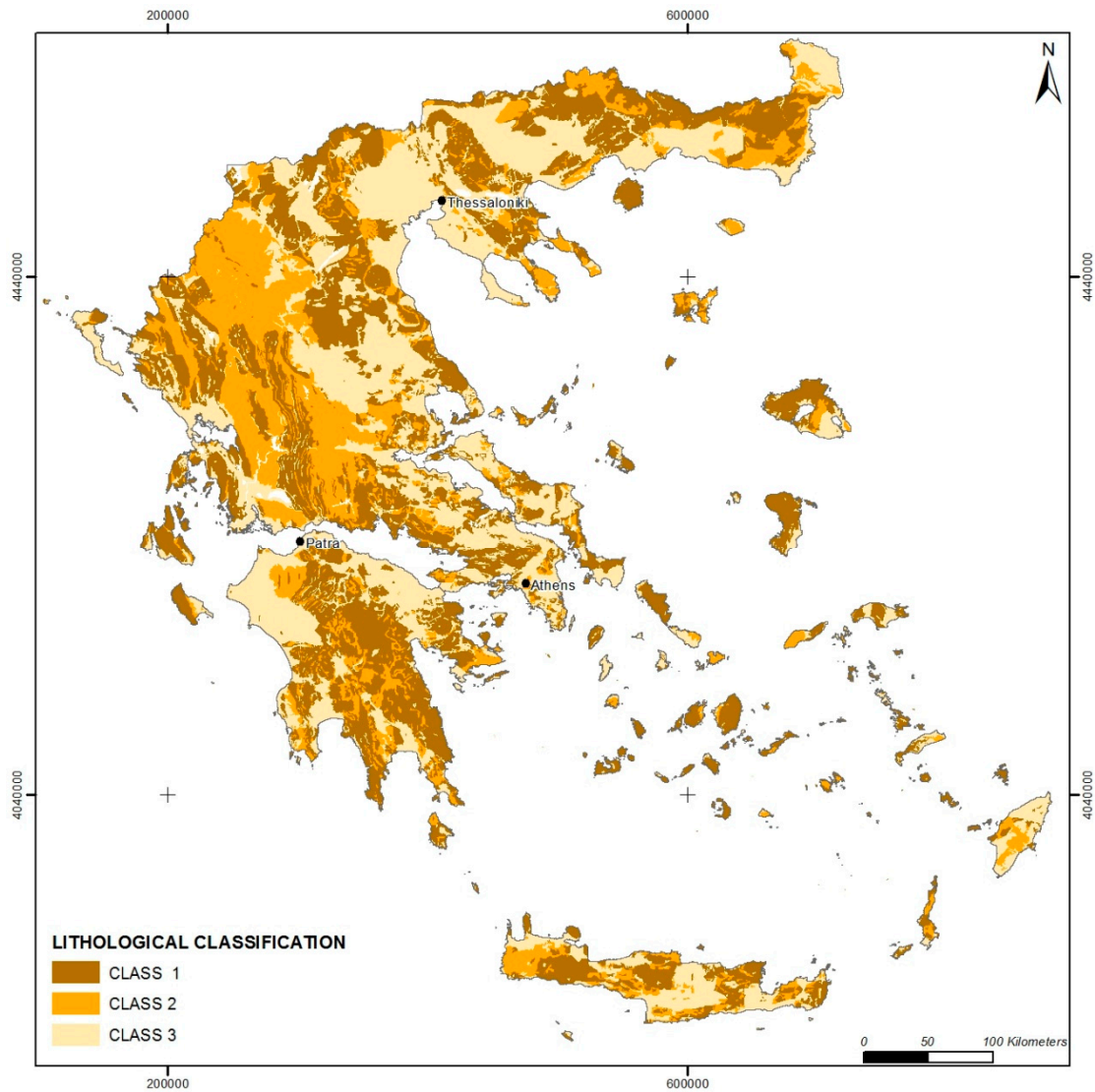


Figure 8. Thematic map of classification of lithology in Greece.

4.2.3. Rainfall intensity

It has been established by many studies that rainfall intensity correlates well with the occurrence of rockfalls. Krautblatter & Moser (2009) proposed a nonlinear model coupling between rainfall and rockfall based on a 4-year monitoring in the Alps. In a number of studies it is suggested, that the maximum precipitation in 24 hour period for a particular return period (50 or 100 years) tend to correlate better with triggering of instability slope phenomena. This is based on the fact that high but regular rainfall tends not to saturate slopes, while lower but irregular rainfall does. Since the assessment is at a national scale, the annual precipitation was chosen for the

correlation with rockfall events. A simple rating was proposed considering that rockfall susceptibility increases with annual rainfall intensity. The rating of rainfall intensity is shown in Table 4. The annual precipitation map (Isohyetal contouring) was prepared at an original scale 1:500.000 (Institute of Geology and Mineral Exploration–IGME) and is presented in Figure 9.

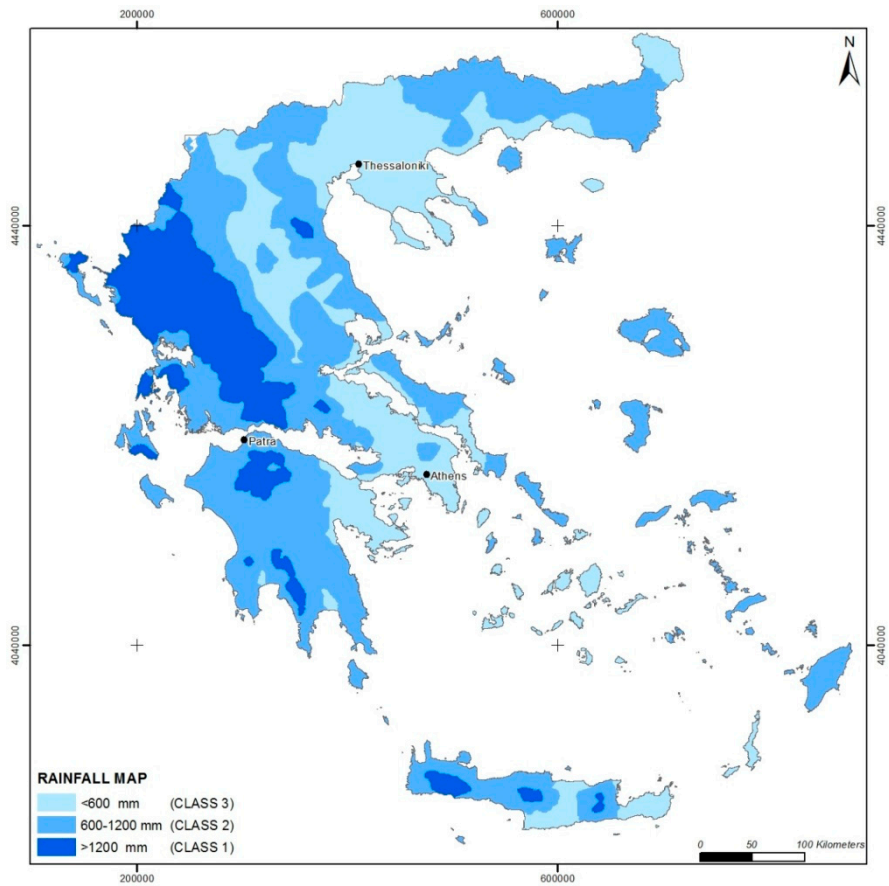


Figure 9. Thematic map of classification of rainfall intensity in Greece.

Table 4. Rating of annual rainfall intensity

Rainfall intensity (height of rainfall per year)	Rockfall susceptibility	Class
< 600 mm	Low	3
600 mm < R < 1200 mm	Moderate	2
> 1200 mm	High	1

4.2.4. Earthquake intensity

Harp & Jibson (2002) proposed that concentrated seismically triggered rockfalls may result from local amplification of seismic shaking. In order to take into account the

effect of earthquakes on the susceptibility, the rating of the acceleration coefficient was considered. Based on the fact that Greece is characterized by three categories with different acceleration coefficients (EPPO, 2003), a simple rating was proposed for earthquake intensity. This rating is summarized in Table 5 and the classification map is presented in Figure 10.

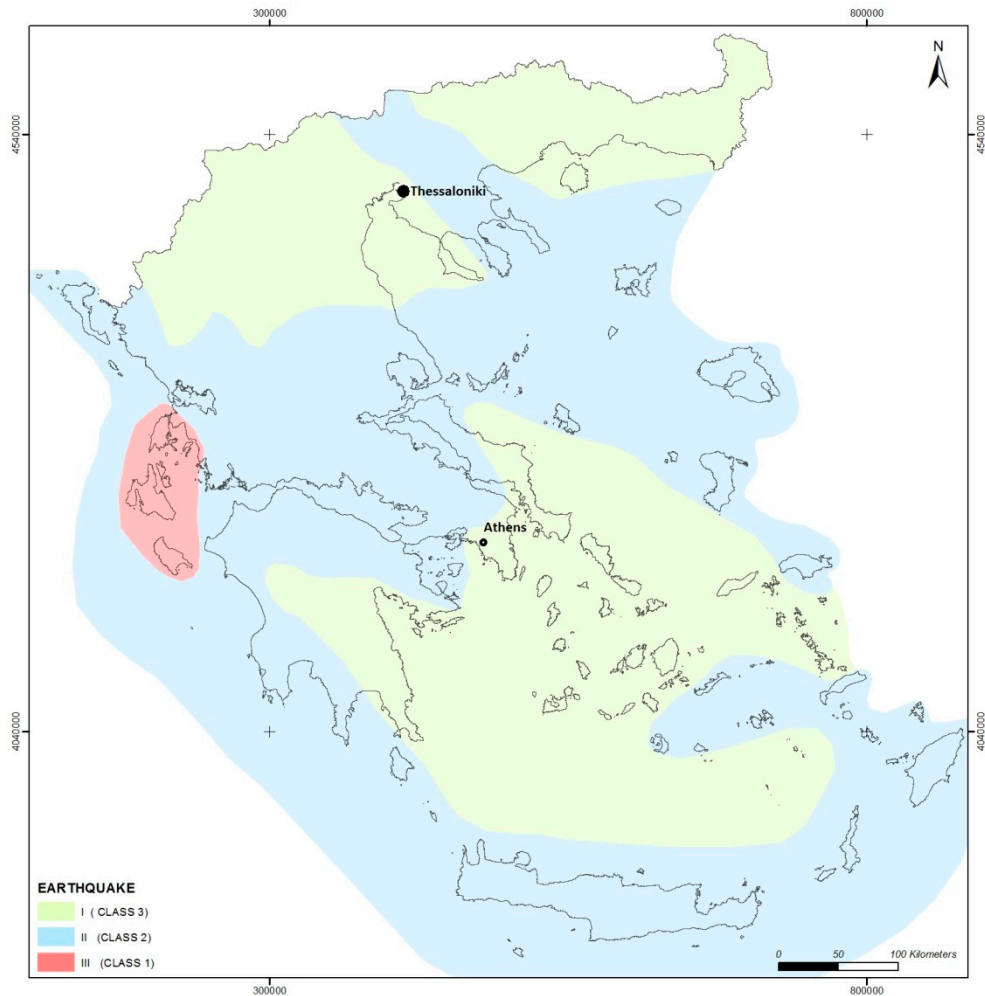


Figure 10. Thematic map of classification of earthquake intensity in Greece.

Table 5. Rating of earthquake intensity

Earthquake intensity	Rockfall susceptibility	Class
< 0.12g	Low	3
0.12g < a < 0.24g	Moderate	2
> 0.24g	High	1

4.2.5. Presence of faults

Fault zones increase rockfall potential by creating steep slopes and weakened, highly fractured rockmasses. The concept of a fault damage zone has been documented by many authors and a general classification has been published by Kim et al. (2004). Shipton and Cowie (2003) observed that the damage zone width is approximately 2.5 times the throw, but added that this value is lithology dependant. Brideau et al. (2005) observed that the block size and shape vary as a function of the distance from a fault. The extent of the damage zones that they observed is up to 10 m.

The major faults and thrusts included in the Greek territory have been digitized from the geological map (IGME, scale 1:500.000) and superimposed to form a vector layer. On this layer, a distance function was applied in order to define buffer zones along the structural discontinuities, while two buffer zones, each one of 250m wide, were created. The basis of this selection was considering that the estimated width of influence by the presence of a fault in terms of increased fracturing of a rockmass is 250 m. In order to account for the fault presence in the rockfall susceptibility rating, a value of 1 is attributed when a fault is present within a distance of 250 m from the rock slope and a value of 0 is attributed when no fault is present.

Based on the inventory, twenty (20) slopes are related to fault presence and this result in higher rockfall activity. Rondoyanni et al. (2013) has highlighted the importance of presence of active faults on highway slopes in Greece.

4.3. SUSCEPTIBILITY MAP

The matrix based approach is described by a simple index, denoted as Rockfall Susceptibility Index (RSI), which is the sum of the class rating of the aforementioned factors according to the following equation:

$$RSI = \sum Lr + Rr + Er + Fr \quad (1)$$

where:

384 RSI – Rockfall susceptibility index

385 Lr – lithology

386 Rr – rainfall intensity

387 Er – earthquake intensity

388 Fr – fault presence

389 Thus, a regional area is more susceptible to rockfalls when the index has lower
 390 values. The slope gradient is not summed in the index RSI and when its value is 0 no
 391 rockfall occurs. Rockfall susceptibility is classified in three categories, "low" ($8 \leq \text{RSI}$
 392 ≤ 9), "moderate" ($5 \leq \text{RSI} \leq 7$) and "high" ($3 \leq \text{RSI} \leq 4$), according to a matrix based
 393 approach for all the possible combinations between the categories of the main
 394 factors. The rating matrix is presented in Table 6. It is highlighted, that each factor
 395 has an equal weight in the calculation of the total susceptibility index.

396 Table 6. Rating matrix for the calculation of Rockfall Susceptibility Index (RSI).
 397 Category of low susceptibility in grey, moderate in green and high in red colour.

RSI	Earthquake (class 1)	Earthquake (class 2)	Earthquake (class 3)
Lithology + Rainfall classes (sum=2)	3	4	5
Lithology + Rainfall classes (sum=3)	4	5	6
Lithology + Rainfall classes (sum=4)	5	6	7
Lithology + Rainfall classes (sum=5)	6	7	8
Lithology + Rainfall classes (sum=6)	7	8	9

398 The spatial distribution of rockfall susceptibility in Greece, based on this approach is
 399 presented in Figure 11. It forms a basis for spatial prediction of the rockfall triggering
 400 areas and it gives a general overview of susceptible areas at a national scale. The
 401 results of this approach cannot be accurate if the susceptibility is examined in a local
 402 scale, since the resolution of the map is quite low for such purposes. Furthermore, it
 403 gives guidance for further and more detailed research studies.

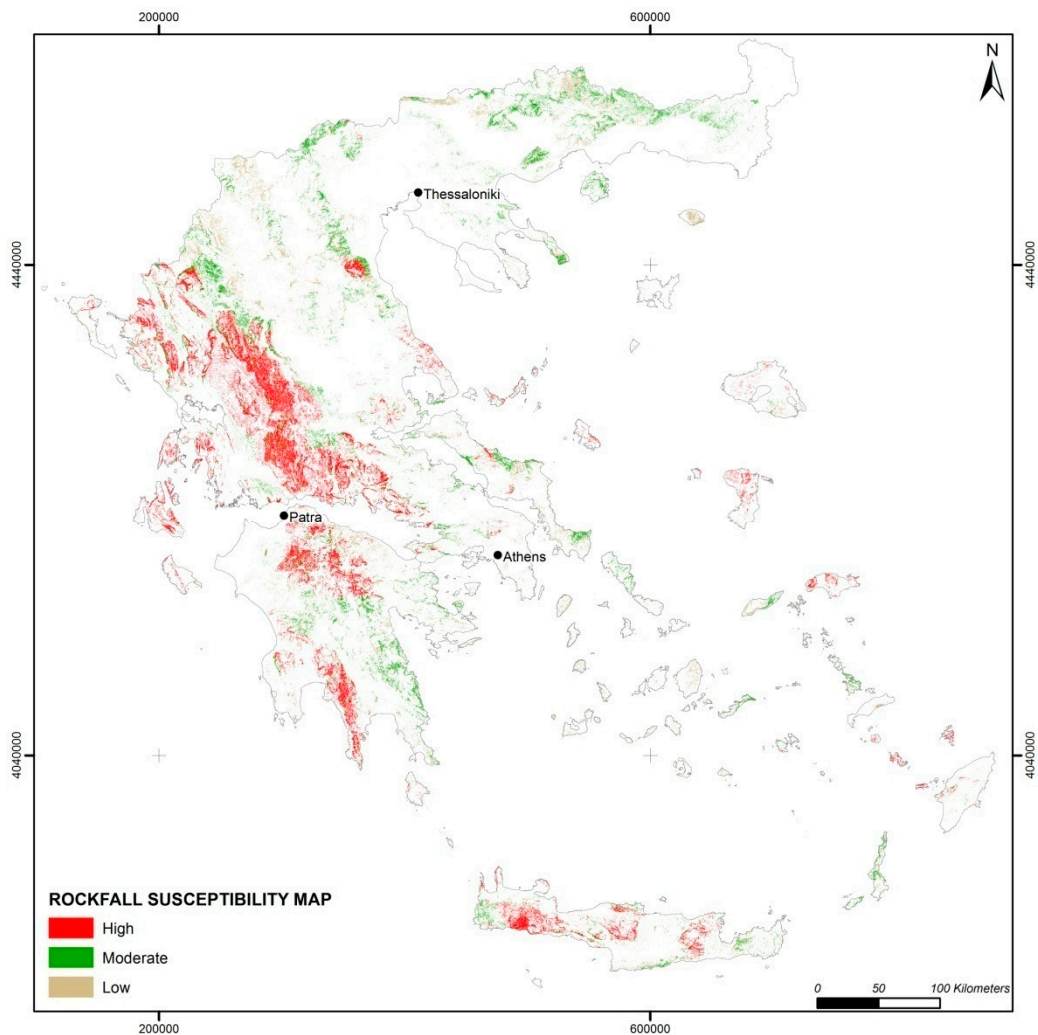


Figure 11. Rockfall susceptibility map of Greece

4.4. **DISCUSSION**

In order to check the reliability of the susceptibility zoning map, the data set of the rockfall inventory presented earlier was used. The susceptibility map accompanied by the locations of the rockfall inventory is shown in Figure 12.

It is evident, that the majority of the recorded events are encountered in areas characterized as moderately to highly susceptible to rockfalls. Some events (locations no. 1, 8, 20, 23 and 37) are encountered in areas with low susceptibility. This is anticipated, as the resolution of the susceptibility map is relatively low and thus cannot accurately predict the occurrence of a rockfalls in regional or local scale. For example, the slope gradient in a small area may be very high due to the

presence of a steep rock slope (such as in location no.1), which is not reflected in the DTM used for the preparation of the susceptibility map.

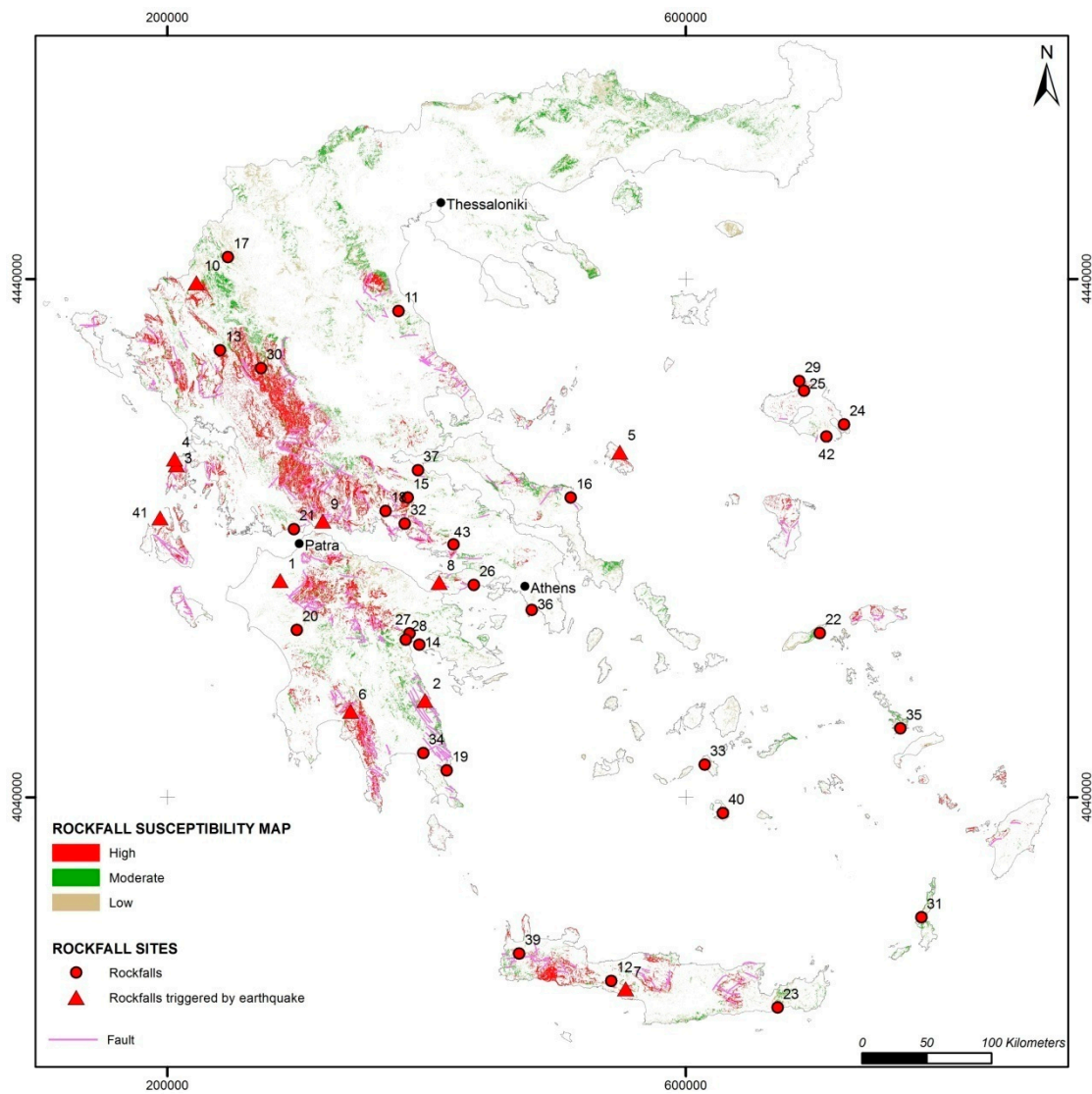


Figure 12. Rockfall susceptibility map and inventory of rockfalls in Greece

5. CONCLUSIONS

According to the results of the present research, a rockfall susceptibility zoning map for Greece was prepared based on a simple Rockfall Susceptibility Index (RSI). This index is based on the rating of the a) slope gradient b) slope lithology, c) rainfall intensity, d) earthquake intensity and e) fault presence. The map forms a basis for spatial prediction of rockfall prone areas at a national scale while it provides guidance for further and more detailed investigation at regional scale. It also represents areas

exposed to rockfalls and provides the first necessary information towards land use decisions by governmental administrations. Another benefit is that it can assist in the detection of human infrastructure located in susceptible areas which require further analysis, such as hazard and risk.

The reliability of the susceptibility zoning map was checked using a data set of sixty (60) rockfall events for the period between 1935 and 2019. A validation against an independent dataset could be carried out in the future, when new data from rockfalls will be available. Based on the analysis of the recorded data from this inventory, it was evident that the number of rockfalls has increased in the recent years.

It was also evident that the main triggering factor was rainfall (33%), while the second most frequent triggering mechanism was earthquake loading (25%). Emphasis was given to investigate the possible presence of faults in rockfall prone areas and it was shown that half of the rockfall events occurred in slopes where fault scarps exist.

The effect of earthquakes as a triggering mechanism, in particular the relation with epicenter distance and magnitude of earthquake, was also studied. It was found that coseismic rockfall events in Greece were triggered with earthquakes of magnitude between $M_w = 5.7$ and 6.7, while the distance from the epicenter to a reported rockfall was between 3 and 37 km.

The impact of rockfalls was severe in most cases, mainly resulting in damages to roads and houses (32% and 20% of the total events respectively) while few events resulted in casualties. The potential risk to archaeological sites is also quite high (11 % of the total events).

The present study was the first comprehensive study on the occurrence of rockfalls in Greece. It provides a susceptibility zoning assessment at a national scale based on the most important factors, which can prove a valuable decision support tool against rockfall hazards.

Acknowledgments

The author would like to thank I.G.M.E. for providing data from technical reports on rock slope instabilities and Dr. I. Kalogeras, National Observatory of Athens for providing data on the studied earthquakes in Greece. The assistance of Mrs. E. Lykoudi in the preparation of GIS maps is gratefully acknowledged.

6. REFERENCES

- Ambraseys N.N. & Jackson J.A. (1990). Seismicity and associated strain of central Greece between 1890 and 1988. *Geophys. J. Int.* 101, pp. 663-708.
- Antoniou A.A., Lekkas E. (2010) "Rockfall susceptibility map for Athinios port, Santorini island, Greece", *Geomorphology*, 118; 152-166.
- Baillifard F., Jaboyedoff M. & Sartori M., (2003). Rockfall hazard mapping along a mountainous road in Switzerland using a GIS-based parameter rating approach. *Natural Hazards and Earth System Sciences*, 3: 431–438.
- Barredo JJ, Benavides A, Hervás J, Van Westen CJ., (2000). Comparing heuristic landslide hazard assessment techniques using GIS in the Trijana basin, Gran Canaria Island, Spain. *JAG2* 1:9-23.
- Brabb EE (1984) Innovative approaches to landslide hazard mapping. In: *Proceedings 4th international symposium on landslides*, Toronto, vol 1, pp 307–324.
- Brideau, M.A., Stead, D., Kinakin, D., Fecova, K., (2005). Influence of tectonic structures on the Hope Slide, British Columbia, Canada. *Engineering Geology* 80, 242–259.
- Calvellido M, Cascini L, Mastroianni S., (2013). Landslide zoning over large areas from a sample inventory by means of scale-dependent terrain units. *Geomorphology* 182: 33-48.
- Carrara A, Cardinali M, Detti R, Guzzetti F, Pasqui V, Reichenbach P., (1991). GIS Techniques and statistical models in evaluating landslide hazards. *Earth Surface Process Landforms* 16:427-445.
- Čarman M, Kumelj S., Komac M., Ribicic M., 2011. Rockfall susceptibility map of Slovenia. *Proceedings of Interdisciplinary Rockfall Workshop*, Innsbruck.

- 483 Chau K.T., Wong R.H.C., Liu J., Lee C.F. (2003). Rockfall hazard analysis for Hong
484 Kong based on rockfall inventory. *Rock Mech. Rock Engng*, 36 (5), 383–408.
- 485 Chau K.T., Tang Y.F., Wong R.H.C., (2004). GIS based rockfall hazard map for Hong
486 Kong, *Int. J. Rock Mech. Min. Sci.*, vol. 41, No.1, p. 846-851.
- 487 Christaras B. & Vouvalidis K. (2010), Rockfalls in the archaeological site of Delphi,
488 Greece. *Proc. of IAEG 2010 International Congress*, Auckland.
- 489 Chousianitis, K., Del Gaudio, V., Sabatakakis, N., Kavoura K., Drakatos, G.,
490 Bathrellos, G. D., Skilodimou, H. D., (2016). Assessment of Earthquake-
491 Induced Landslide Hazard in Greece: From Arias Intensity to Spatial
492 Distribution of Slope Resistance Demand. *Bull. of the Seismological Society of*
493 *America*, Vol. 106, No. 1, pp. 174–188.
- 494 Coe J.A., Harp E.L., (2007). Influence of tectonic folding on rockfall susceptibility,
495 American Fork Canyon, Utah, USA. *Nat. Hazards Earth Syst. Sci.*, 7, 1–14.
- 496 Dorren L. Seijmonsbergen A., (2003). Comparison of three GIS-based models for
497 predicting rockfall runout zones at a regional scale. *Geomorphology*, vol. 56,1-
498 2, p.49–64.
- 499 EPPO, (2003). Greek seismic code. Earthquake Planning and protection
500 Organization, Athens.
- 501 Fell R., Corominas J, Bonnard C, Cascini L., Leroi E., Savage W.Z. (2008)
502 Guidelines for landslide susceptibility, hazard and risk-zoning for land use
503 planning. *Engineering Geology* 102, 85-98.
- 504 Ferrari F., Giacomini A., Thoeni K. (2016). Qualitative rockfall hazard assessment: A
505 comprehensive review of current practices. *Rock Mech Rock Eng.* DOI
506 10.1007/s00603-016-0918-z
- 507 Fernandez T, Irigaray C, Hamdouni RE, Chacon J., (2003). Methodology for
508 landslide susceptibility mapping by means of a GIS, application to the
509 Contraviesa Area (Granada, Spain). *Natural hazards* 30:297-308.
- 510 Fityus, S.G., Giacomini, A., Buzzi, O., (2013). The significance of geology for the
511 morphology of potentially unstable rocks, *Eng. Geol.*, doi:
512 10.1016/j.enggeo.2013.05.007.
- 513 Gorum T., Fan X., J. van Westen C., Huang R. Q., Xu Q., Tang C., Wang G., (2011).
514 Distribution pattern of earthquake-induced landslides triggered by the 12 May
515 2008 Wenchuan earthquake. *Geomorphology*, 133, p. 152-167.

- 516 Gupta, R. P., Saha, A. K., Arora, M. K., and Kumar A., (1999). Landslide Hazard
517 Zonation in part of the Bhagirathi Valley, Garhwal Mimalyas, using integrated
518 remote sensing – GIS. *Himalayan Geology*, 20, 71–85.
- 519 Guzzetti F, Reichenbach P, Ardizzone F, Cardinali M, Galli M (2006) Estimating the
520 quality of landslide susceptibility models. *Geomorphology* 81:166–184.
- 521 Günther, A., Reichenbach, P., Malet, J. P., Van Den Eeckhaut, M., Hervás, J.,
522 Dashwood, C., & Guzzetti, F. (2013). Tier-based approaches for landslide
523 susceptibility assessment in Europe. *Landslides*, 10(5), 529-546.
- 524 Harp, E.L., Jibson, R.W., (2002). Anomalous concentrations of seismically triggered
525 rock falls in Pacoima Canyon: Are they caused by highly susceptible slopes or
526 local amplification of seismic shaking. *Bulletin of the Seismological Society of*
527 *America*, v. 92, no. 8, p. 3,180–3,189.
- 528 Institute of Geology and Mineral Exploration. Geological map of Greece (scale
529 1:500.000).
- 530 Keefer, D. K. (1984) Landslides caused by earthquakes, *Bull. Geol. Soc. Am.*, 95,
531 406–421.
- 532 Kim, Y.-S., Peacock, D.C., Sanderson, D.J., (2004). Fault damage zones. *Journal of*
533 *Structural Geology* 26, 503–517.
- 534 Kolat C, Doyuran V, Ayday C, Suzen ML., (2006). Preparation of a geotechnical
535 microzonation model using GIS Systems based on Multicriteria decision
536 Analysis. *Eng Geol.* 87:241-255.
- 537 Koukis G., Ziourkas C. (1991). Slope instability phenomena in Greece: A statistical
538 analysis. *Bull. Int. Assoc. Eng. Geology*, vol. 43, 47-60.
- 539 Koukis G, Sabatakakis N, Nikolaou N, Loupasakis C (2005) Landslide hazard
540 zonation in Greece. In: Sassa K, Fukuoka H, Wang F, Wang G (eds) *Proc. 1st*
541 *General Assembly and The 4th Session of Board of Representatives of the Int.*
542 *Consortium on Landslides*, pp. 291–296.
- 543 Koukouvelas I., Litoseliti A., Nikolakopoulos K., Zygouri V. (2015). Earthquake
544 triggered rock falls and their role in the development of a rock slope: The case
545 of Skolis Mountain, Greece. *Engineering Geology*, 191, 71–85.
- 546 Krautblatter M., Moser, M., (2009). A nonlinear model coupling rockfall and rainfall
547 intensity based on a four year measurement in a high Alpine rock wall (Reintal,
548 German Alps). *Nat. Hazards Earth Syst. Sci.*, 9, 1425–1432.

- 549 Mancini F, Ceppi C, Ritrovato G, (2010). GIS and statistical analysis for landslide
550 susceptibility mapping in the Daunia area, Italy. *Nat Haz Earth Syst Sci*, 10:
551 1851–1864.
- 552 Marinos P., Kavvadas M., Tsiambaos G., Saroglou H., (2002). Rock slope
553 stabilization in Mythimna castle, Lesbos island, Greece. *Proc. 1st European*
554 *conference on landslides*, Balkema, Rybar Stemberk & Wagner (eds), Prague,
555 635-639.
- 556 Marinos P, Tsiambaos G., (2002). Earthquake triggering rock falls affecting historic
557 monuments and a traditional settlement in Skyros Island, Greece. *Proc. of the*
558 *Int. Symposium: Landslide risk mitigation and protection of cultural and natural*
559 *heritage*, Kyoto, Japan, pp. 343-346.
- 560 Marquínez J., Menéndezduarte R., Farias P. & Jiménez Sánchez M. (2003).
561 Predictive GIS-based model of rockfall activity in mountain Cliffs. *Natural*
562 *Hazards* 30: 341–360.
- 563 Marzorati S., Luzi L., De Amicis M., (2002). Rock falls induced by earthquakes: a
564 statistical approach. *Soil Dynamics and Earthquake Engineering*, 22, 565-577.
- 565 Mason, P.J., Rosenbaum, M.S., (2002). Geohazard mapping for predicting landslides:
566 an example from the Langhe Hills in Piemonte, NW Italy. *Quarterly Journal of*
567 *Engineering Geology and Hydrogeology* 35:317-326.
- 568 Meisina, C., Piccio, A., and Tocchio, A. (2001): Some aspects of the landslide
569 susceptibility in the Sorba Valley (western Alps, Italy), in: *Int. Conf. on*
570 *Landslides – Causes, Impacts and Countermeasures*, Kuhne, M., Einstein, H.
571 H., Krauter, E., Klapperich, H., and Pottler, R. (eds.), Davos, Switzerland, VGE,
572 Essen, 547–556.
- 573 Nandi, A., Shakoor, A., (2009). A GIS-based landslide susceptibility evaluation using
574 bivariate and multivariate statistical analyses. *Eng Geol* 110:11-20.
- 575 Nikolaou N., Pogiati E., Spanos N. (2011) Report on landslides in Greece on 2010,
576 I.G.M.E. p.8.
- 577 Papadopoulos GA, Plessa A., (2000). Magnitude–distance relations for earthquake–
578 induced landslides in Greece. *Eng Geol* 58(3–4): 377–386.
- 579 Papathanassiou, G., Valkaniotis, S., Ganas, A. and Pavlides, S., (2013). GIS-based
580 statistical analysis of the spatial distribution of earthquake - induced landslides
581 in the island of Lefkada, Ionian Islands, Greece, *Landslides*, 10, 771-783.

- 582 Papazachos, B.C., Papazachou, C., (1997). The Earthquakes of Greece. Editions
583 ZITI, Thessaloniki. 304 pp.
- 584 Paulin GL, Bursik M, Hubp JL, Mejia LMP, Quesada FA, (2014). A GIS method for
585 landslide inventory and susceptibility mapping in the Rio El Estado watershed,
586 Pico de Orizaba volcano, Mexico. *Nat Hazards* 71:229-241.
- 587 Pavlides & Caputo (2004). Tectonophysics Magnitude versus fault's surface
588 parameters: quantitative relationships from the Aegean Region.
589 *Tectonophysics*, 380, 3-4, 159-188.
- 590 Rodriguez, C. E., Bommer, J. J., and Chandler, R. J. (1999) Earthquake induced
591 landslides: 1980–1997, *Soil Dyn. Earthq. Eng.*, 18, 325–346.
- 592 Rodriguez -Peces M. J., Garcia-Mayordomo J., Azanon J., Jabaloy A., (2011).
593 Regional Hazard Assessment of Earthquake-Triggered Slope Instabilities
594 considering Site Effects and Seismic Scenarios in Lorca Basin (Spain).
595 *Environmental & Engineering Geoscience*, Vol. XVII, No. 2, May 2011, pp.
596 183–196.
- 597 Rondoyanni T., Lykoudi E., Triantafyllou A., Papadimitriou M., Foteinos I. (2013)
598 Active faults affecting linear engineering projects: Examples from Greece.
599 *Geotech Geol Eng*, 31, 1151-1170.
- 600 Sabatakakis N., Koukis G., Vassiliades E., Lainas S. (2013). Landslide susceptibility
601 zonation in Greece. *Nat. Hazards*, 65: 523-543.
- 602 Saroglou, H., Marinos, V., Marinos, P., Tsiambaos, G. (2012). Rockfall hazard and
603 risk assessment: an example from a high promontory at the historical site of
604 Monemvasia, Greece. *Natural Hazards and Earth System Sciences*, 12, 1823–
605 1836. doi:10.5194/nhess-12-1823-2012.
- 606 Saroglou, H. (2013). Rockfall hazard in Greece. *Bulletin of the Geological Society of*
607 *Greece*, vol. XLVII, no3, 1429-1438.
- 608 Saroglou H., Berger F., Bourrier F., Asteriou P., Tsiambaos G., Tsagkas D. (2015).
609 Effect of forest presence on rockfall trajectory. An example from Greece. *Proc.*
610 *12th Int. Congress of IAEG, Torino. Engineering Geology for Society and*
611 *Territory-Volume 2*, 1899-1903.
- 612 Saroglou H., Asteriou P., Tsiambaos G., Manousakis J., Zekkos D. (2017). Study of
613 co-seismic rockfalls during Lefkada and Cephalonia Earthquakes, Greece.

- 614 Proc. of 3rd North American Symposium on Landslides, Virginia, USA.
615 Association of Environmental & Engineering Geologists (AEG), pp. 521-528.
- 616 Saroglou, H., Asteriou, P., Zekkos, D., Tsiambaos, G., Clark, M., and Manousakis, J.
617 (2018). UAV-based mapping, back analysis and trajectory modeling of a
618 coseismic rockfall, *Nat. Hazards Earth Syst. Sci.*, 18, 321–333.
- 619 Sartori, M., Baillifard, F., Jaboyedoff, M., Rouiller, J.-D., (2003). Kinematics of the
620 1991 Randa rockslides (Valais, Switzerland), *Nat. Hazards Earth Syst. Sci.*, 3.
- 621 Shipton, Z.K., Cowie, P.A., (2003). A conceptual model for the origin of fault damage
622 zone structures in high-porosity sandstone. *Journal of Structural Geology* 25,
623 333–344.
- 624 Trigila, A., Frattini, P., Casagli, N., Catani, F., Crosta, G., Esposito, C., Iadanza, C.,
625 Lagomarsino D., Mugnozza G.S., Segoni S., Spizzichino D., Tofani V., Lari S.
626 (2013). Landslide susceptibility mapping at national scale: the Italian case
627 study. In *Landslide science and practice*, pp. 287-295. Springer, Berlin,
628 Heidelberg.
- 629 Wasowski, J., Del Gaudio V., (2000). Evaluating seismically induced mass
630 movement hazard in Caramanico Terme (Italy). *Eng. Geol.*, 58, 291-311.
- 631 Yilmaz, I., Yildirim, M. (2006). Structural and geomorphological aspects of the Kat
632 landslides (Tokat-Turkey) and susceptibility mapping by means of GIS. *Environ*
633 *Geol* 50:461-472.
- 634 Zygori, V. and Koukouvelas, I.K., 2015. Evolution of rock falls in the Northern part of
635 the Peloponnese, Greece, IOP, Conference series: Earth and Environmental,
636 26, 012043, Warwick UK, 10-11 September, doi:10.1088/1755-
637 1315/26/1/012043